Modulation of the Peri-Infarct Neurogliovascular Function by Delayed COX-1 Inhibition

Evelyn M.R. Lake, PhD,[1,2]* James Mester, BSc,[2] Lynsie AM Thomason, MSc,[3] Conner Adams, BSc,[2] Paolo Bazzigaluppi, PhD,[3,4] Margaret Koletar, BSc,[3] Rafal Janik, MSc,[2,3] Peter Carlen, MD,[4] JoAnne McLaurin, PhD,[5,6,7] Greg J Stanisz, PhD,[2,3,8] and Bojana Stefanovic, PhD[2,3,7]

Purpose: Stroke is the leading cause of adult disability worldwide. The absence of more effective interventions in the chronic stage—that most patients stand to benefit from—reflects uncertainty surrounding mechanisms that govern recovery. The present work investigated the effects of a novel treatment (selective cyclooxygenase-1, COX-1, inhibition) in a model of focal ischemia.

Materials and Methods: FR122047 (COX-1 inhibitor) was given beginning 7 days following stroke (cortical microinjection of endothelin-1) in 23 adult male rats. Longitudinal continuous-arterial-spin-labeling was performed prior to treatment (7 days), and repeated following treatment (21 days) on a 7T magnetic resonance imaging (MRI) system to estimate resting perfusion and reactivity to hypercapnia. These in vivo measurements were buttressed by immunohistochemistry.

Results: Stroke caused an increase in perilesional resting perfusion (peri-/contralesional perfusion ratio of $170 \pm 10\%$) and perfusion responses to hypercapnia ($180 \pm 10\%$) at 7 days. At 21 days, placebo-administered rats showed normalized perilesional perfusion ($100 \pm 20\%$) but persistent hyperreactivity ($190 \pm 20\%$). Treated animals exhibited sustained perilesional hyperperfusion ($180 \pm 10\%$). Further, reactivity lateralization did not persist following treatment (peri- vs. contralesional reactivity: $P = 0.002$ at 7 vs. $P = 0.2$ at 21 days). Hemodynamic changes were accompanied by neuronal loss, increased endothelial density, and widespread microglial and astrocytic activation. Moreover, relative to controls, treated rats showed increased perilesional neuronal survival ($22 \pm 1\%$ vs. $14.9 \pm 0.8\%$, $P = 0.02$) and decreased microglia/macrophage recruitment ($17 \pm 1\%$ vs. $20 \pm 1\%$, $P = 0.05$). Finally, perilesional perfusion was correlated with neuronal survival (slope $= 0.14 \pm 0.05$; $R^2 = 0.7$, $P = 0.03$).

Conclusion: These findings shed light on the role of COX-1 in chronic ischemic injury and suggest that delayed selective COX-1 inhibition exerts multiple beneficial effects on the neurogliovascular unit.

Level of Evidence: 1

Technical Efficacy: Stage 4

J. MAGN. RESON. IMAGING 2017;46:505–517

To date, the majority of stroke treatment research has focused on acute treatment strategies,[1] yet most patients arrive at a care facility beyond the window of opportunity for recanalization.[2] The development of more effective chronic-stage treatments is predicated on furthering our understanding of the cellular mechanisms that govern long-term recovery. In situ functional neuroimaging in animal models is particularly useful in this respect, as it enables longitudinal examination of the spatiotemporal evolution of changes in the morphology and function of the neurogliovascular unit in well-controlled conditions.

View this article online at wileyonlinelibrary.com. DOI: 10.1002/jmri.25541

Received Jul 31, 2016, Accepted for publication Oct 20, 2016.

*Address reprint requests to: E.M.R.L., Yale University School of Medicine, Anlyan Center, N134, 300 Cedar St., New Haven, CT, 06519. E-mail: lakeevelyn@gmail.com

From the [1]Department of Radiology and Biomedical Imaging, Yale University, New Haven, Connecticut, USA; [2]Department of Medical Biophysics, University of Toronto, Ontario, Canada; [3]Physical Sciences, Sunnybrook Research Institute, Toronto, Ontario, Canada; [4]Fundamental Neurobiology, Toronto Western Research Institute, Toronto, Ontario, Canada; [5]Biological Science, Sunnybrook Research Institute, Toronto, Ontario, Canada; [6]Department of Laboratory Medicine and Pathobiology, University of Toronto, Ontario, Canada; [7]Heart and Stroke Foundation Canadian Partnership for Stroke Recovery, Ottawa, Ontario, Canada; and [8]Department of Neurosurgery and Pediatric Neurosurgery, Medical University, Lublin, Poland

Additional Supporting Information may be found in the online version of this article.

A prominent pathophysiological consequence of stroke is inflammation, comprising leukocyte infiltration, activation, and accumulation of microglia, macrophages, and astrocytes, and an increased production of inflammatory mediators.[3] Hitherto, candidate antiinflammatory therapeutics have been preponderantly applied within the acute period. Chronically, inflammatory processes evolve and exert both deleterious and beneficial effects on remodeling and repair.[4] Following stroke, a hypoxia-induced increase in intracellular Ca^{2+} raises the production of arachidonic acid (AA).[5] Cyclooxygenases (COX-1 and COX-2) metabolize AA to different bioactive prostaglandins (PGs).[6] Some PGs ameliorate excitotoxicity[7,8] while others activate polyadenosine diphosphate (ADP) ribose polymerase (PARP) and caspase-3, causing an accumulation of ubiquitinated proteins and contributing to neuronal apoptosis.[9] Select PGs regulate blood vessel tone[10] acting as either vasodilators or constrictors,[11] control platelet aggregation,[6] and affect leukocyte activation and leukocyte-endothelial interactions.[11]

Although promising effects have been observed with COX-2 inhibition in the acute stage of stroke in preclinical research,[6] long-term placebo-controlled clinical studies have revealed serious cardiovascular side effects of COX-2 inhibitors.[12–14] In view of these challenges, attention has begun to turn to downstream PGs as well as to selective COX-1 inhibition.[6,15] Indeed, several PGs that ameliorate excitotoxicity in humans, but not necessarily rodents, derive from COX-2 activity.[6,16] In addition, PGs that act as vasodilators and antithrombotic agents are predominantly produced by COX-2 (in humans and rodents).[11] On the other hand, a number of PGs that promote neuronal apoptosis,[9] constrict vessels, and promote platelet aggregation[6] are preponderantly produced by COX-1 in humans and rodents.[17,18] Notwithstanding, few studies have investigated the role of COX-1 in the pathogenesis of stroke, especially in the chronic stage, and the available data on the (sub)acute period are conflicting.[6,15] COX-1 null mice have been shown to exhibit a greater reduction in perilesional blood flow 4 days poststroke and increased ischemic injury.[19] In contrast, a single intraperitoneal dose of valeryl salicylate, a COX-1 inhibitor, 6 hours following ischemia attenuated inflammation, neuronal loss, and oxidative stress on postmortem histology in a gerbil model of transient global ischemia.[20] Moreover, COX-1 inhibitors are particularly attractive given their long-standing safety record and widespread use in managing inflammation. To investigate the role of COX-1 in the chronic stage of stroke, we assessed cerebrovascular function, inflammation, and neuronal survival, following the administration of FR122047, a highly selective COX-1 antagonist.

Materials and Methods

All experimental procedures in this study adhered to the guidelines specified by Animal Research Reporting In Vivo Experiments (ARRIVE) and were approved by the Animal Care Committee at the facility where experiments were performed, which adheres to the Policies and Guidelines of the Canadian Council on Animal Care and meets all the requirements of the Provincial statute of Ontario, Animals for Research Act, as well as those of the Federal Health of Animals Act. All data processing was performed blinded to group allocation (placebo or FR122047) and time postischemia (7 vs. 21 days). Animals were housed in pairs in Allentown Micro-Vent cages (at 21°C) on a reverse 12-hour light/dark cycle (all procedures and imaging were performed during the dark phase). Animals remained in home cages for the duration of this study where food (standard chow) and water were freely available. During all surgical procedures (which were performed under aseptic conditions) and imaging sessions, body temperature, breath rate, heart rate, and blood oxygen saturation were monitored continuously and kept within physiological range (Supplementary Table 1). Animals were euthanized by an overdose of anesthesia.

Inclusion/Exclusion Criteria

Twenty-three adult male Sprague-Dawley rats (Harlan Laboratories, Madison, WI) weighing 297 ± 23 g (mean $\pm$ SD) were included in this study. Three rats went into respiratory arrest and died during endothelin-1 injection. Hardware failure resulted in the death of one rat during the hypercapnic challenge in MRI 7 days after stroke induction; one rat died during ALZET minipump implantation from intracranial bleeding following catheter misplacement, and one rat was euthanized for excessive weight loss (>10% decrease from prestroke body weight) between imaging sessions. Finally, one FR122047-treated rat was excluded at the 21-day imaging session because the catheter used for FR122047 delivery had detached from the skull. Consequently, there were $n = 19$ ($n = 9$ placebo, and $n = 10$ FR122047-treated) MRI datasets collected at 7 days (prior to intervention); and $n = 16$ ($n = 7$ placebo, and $n = 9$ FR122047-treated) at 21 days (postintervention) (see Supplementary Table 2 for animal numbers summary). No modifications to the protocol were made.

Stroke Induction

Stroke was produced by intracortical microinjection of endothelin-1 into sensorimotor cortex of adult rats so as to emulate the kinetics of flow impairment observed in human stroke, and produce a lesion of similar relative volume and composition (with substantial peri-infarct zone surrounding the necrotic core) as seen in many patients.[21,22]

All rats ($n = 23$) underwent the same stroke induction procedure under isoflurane anesthesia (5% induction and 2–2.5% maintenance). Rats were secured in a small rat stereotaxic apparatus (David Kopf Instruments, Tujunga, CA). A midline incision was made, and two burr holes, 0.8 mm in diameter, drilled at 0.0 mm AP (anterior–posterior), –2.5 mm ML (medial–lateral); and at 2.3 mm AP, –2.5 mm ML over the right sensorimotor cortex using a high-speed micro-drill (Foredom Electric, Bethel, CT). A 10-μl Hamilton Syringe (Reno, NV) was used to inject 800 pmol of endothelin-1 (Sigma-Aldrich, St. Louis, MO) suspended in 4 μl of sterile water at –2.3 mm DV (dorsal–ventral). One 2-μl aliquot was injected at each location, for a total of 4 μl. After lowering the needle to –2.5 mm and retracting it to –2.3 mm DV, a 1-minute

delay was allowed before injection began. A further 1-minute delay was kept between the delivery of each μl, and a 2-minute delay preceded needle retraction. Injections were made at a rate of 1 μl/min, for a total delivery time (including four 1-minute delays, and two 2-minute delays) of 12 minutes. Burr holes were closed with bone wax and the scalp sutured over the skull. For analgesia, rats were given a subcutaneous dose of Lidocaine (0.2 mg/kg) at the beginning and end of surgery.

FR122047 Administration

FR122047 was delivered intracerebroventricularly to reduce off-target effects due to the expression of COX-1 throughout the body.[15] All rats were anesthetized with isoflurane (5% induction and 2–2.5% maintenance) and implanted with ALZET-osmotic pumps (ALZET Osmotic Pumps, Cupertino, CA) 7 days after stroke. In preparation, 24–48 hours prior to implantation, ALZET-osmotic pumps (2ML2, delivery rate 5 μl/hr) were loaded with 1.6 mg FR122047 (Cedarlane Laboratories, Burlington, ON, Canada) suspended in 2 ml of sterile saline (dosage of $\sim$400 μg/kg/day) or sterile saline alone (placebo). Superglue (Loctite, Westlake, OH) was used to secure $\sim$8 inches of PV-56 tubing (BTPE-50 polyethylene tubing, Instech Laboratories, Polymouth Meeting, PA) to each ALZET-osmotic pump flow moderator to serve as a delivery catheter. Rats were randomly assigned to either FR122047-treated or placebo (two groups).

A filled pump was inserted into the peritoneal cavity and the musculoperitoneal layer and peritoneal wall were closed leaving the PV-56 tubing catheter penetrating the abdominal cavity at the anterior end of the incision. Using blunt dissection, the cutaneous layer was separated from underlying tissue to allow the catheter to be fed subcutaneously from the abdomen to the base of the skull. At this point, rats were transferred to a stereotaxic apparatus (David Kopf Instruments). Using a high-speed micro-drill (Foredom Electric), a burr hole was made through the interparietal bone 2-mm posterior of lambda and 2-mm right of the midline. The catheter was placed through the burr hole within the lateral ventricle of the right hemisphere and secured to the skull with superglue. For analgesia, rats were given a subcutaneous dose of Lidocaine (0.2 mg/kg) at each incision site at the beginning and at the end of surgery. All incisions were closed with 4.0 absorbable sutures (UNIFY PGA sutures, AD Surgical, Sunnyvale, CA).

Twelve days following pump implantation, all rats underwent the ALZET-osmotic pump extraction procedure (prior to the second MRI session). With the rat in the prone position, a 1-cm midline incision was made at the base of the skull in the M-L direction to access the catheter. The catheter was cut and sealed (with superglue) leaving 1-cm of tubing still within and attached to the back of the skull. The incision overlying the base of the skull was sutured. The ALZET-osmotic pump and attached catheter were next removed from the abdominal cavity. Lidocaine (0.2 mg/kg) was administered subcutaneously at each incision site (Supplementary Fig. 1). Animals were monitored closely (twice daily) for 72 hours postsurgery (stroke induction and pump implantation/removal). Thereafter, the surgical area was inspected daily to look for signs of inflammation/infection. No instances of infection were observed. Frequent postoperation checks of weight, grooming, and behavior were performed. The delivery of FR122047 was verified by measuring the volume loaded into each ALZET-pump (2 ml) prior to implantation, and subsequently quantifying the volume remaining in each pump upon its removal (450 ± 30 μl). We were thereby able to verify that $\sim$1.5 ml of FR122047 or vehicle was delivered to each animal. Further, catheter placement was visualized in all animals on T_2-weighted MRI (Supplementary Fig. 1).

MRI

All rats were imaged 7 and 21 days following stroke on a 7T MRI (Bruker, BioSpec, Etlingen, Germany) using a birdcage body coil for radiofrequency (RF) excitation and a quadrature receive-only coil for signal detection. Rats were immobilized with ear bars and an incisor bar, and a stable plane of anesthesia was maintained with an intravenous infusion of 45 mg/kg/hr of propofol (Pharmascience, Montreal, Quebec, Canada). In the present work, titration experiments have shown that a low dose of propofol (45 mg/kg/hr) is well tolerated and yields robust responses to hypercapnia as well as rapid recovery. Furthermore, animals were intubated and mechanically ventilated with 31% O_2 and 69% N_2. Following the first imaging session, rats were extubated and recovered.

STRUCTURAL IMAGING. Forty-five coronal images were obtained using a rapid acquisition with relaxation enhancement (RARE) sequence (RARE factor of 8, TR/TE of 5500/47 msec, and a matrix size of 128 $\times$ 256), with a nominal in-plane spatial resolution of 0.1 $\times$ 0.1 mm^2 and a slice thickness of 0.5 mm in under 12 minutes. Images were imported into ImageMagick[23] for semiautomated segmentation. Following previous work, voxels with signal more than 2 SD above the mean signal in the corresponding contralesional region of interest (ROI) were classified as perilesional tissue[24,25] (see Supplementary Table 3 for all lesion volumes).

CONTINUOUS ARTERIAL SPIN LABELING (CASL) FMRI ACQUISITION. A custom-built labeling coil was positioned at the level of the carotid arteries, with a quadrature receive-only coil used for signal detection. Following a 1.5-second adiabatic labeling pulse and a 0.4-second postlabeling delay, single-average, single-shot echo-planar images were obtained from five 1.5-mm thick coronal slices positioned over the sensorimotor cortex, with a 0.25 $\times$ 0.25 mm^2 nominal in-plane resolution, and TR/TE of 2000/8.3 msec with a slice gap or 0.5 mm. Vessel reactivity was estimated by repeatedly challenging the rats with 10% CO_2, with inspired mixture composition controlled by a GSM-3 GasMixer (CWE, Boston, MA) in ON:OFF periods of 1:3 minutes (ON: 10% CO_2, 31% O_2, and 59% N_2, OFF: 0% CO_2, 31% O_2, and 69% N_2) for a total acquisition time of 16 minutes.

CASL DATA PROCESSING. All CASL data were motion-corrected (AFNI, Analysis of Functional NeuroImages, 2dImReg), masked (to isolate gray matter), and spatially blurred within the gray matter mask (AFNI 3dBlurInMask, full-width half-maximum 0.55 mm) prior to fitting the data using a Generalized Linear Model (AFNI 3dDeconvolve). Subject-specific hemodynamic response functions were produced by averaging the signal in the left (notionally unaffected) cortical gray matter across all four hypercapnic challenges time-locked to the onset of the increase in the animal's end-tidal CO_2 trace measured by capnography (Capnograph, MicroCapStar, CWE, Ardmore, PA).[26] The capnograph

was programmed to deliver 1-minute-long 10% CO_2 challenges in alternation with 3-minute-long periods of 0% CO_2. Respiration rate was kept constant at 60 breaths per minute using the ventilator and was monitored independently with MouseOx using pulse-oximetry. Physiological monitoring (including breath rate) and output from the capnograph (expired CO_2) were recorded with BioPac. Recording of physiological measurements (by MouseOx and BioPac) was time-locked to the beginning of the MRI acquisition by a digital trigger sent from the MRI scanner to the BioPac software.

A threshold was applied to resulting maps of perfusion signal changes elicited by hypercapnia and resting perfusion to correct for multiple comparisons (false-discovery rate $q < 0.01$). In each animal, we manually identified a training set of ~40–60 voxels in both perfusion response and resting perfusion maps residing in the contralesional and perilesional cortices. The pial surface and boundary with corpus callosum were excluded, along with major vessels. Using these training data, classification was performed with a probabilistic classifier (MINCTools Classify) and thresholds applied to the resulting probabilistic maps: at >80% a posteriori probability of belonging to the healthy left cortex (contralesional ROI) and at >75% a posteriori probability of belonging to the affected right cortex (perilesional ROI).

Immunohistochemistry

Following the final MRI session, rats were perfused with phosphate-buffered saline (PBS) and brains extracted, placed in paraformaldehyde (PFA, Sigma-Aldrich), and stored at 4°C. After 24 hours in PFA, brains were rinsed in PBS and transferred to a 15% sucrose solution initially, and to a 30% sucrose solution 48 hours thereafter (Sigma-Aldrich). In each of the brain specimens analyzed immunohistochemically: the collected sections were evenly spaced within the boundaries of the ischemic injury (defined by hyperintensity on in vivo T_2-weighted images), between 3.0 mm and –0.6 mm from Bregma in the A-P direction. The fractional area occupied by stained cells was computed and compared between groups.

For each primary antibody, six evenly spaced free-floating 40-μm coronal sections were collected within the boundaries of the ischemic injury. Sections were singly labeled with primary antibodies, followed with secondary antibodies conjugated with Alexa 488 fluorescent dye (1/200, goat antirabbit A-11008, goat antimouse A-11001, ThermoFisher Scientific, Calgary, Alberta, Canada). The primary antibodies used were: NeuN (1/200, MAB377, EMD Millipore, Billerica, MA), RECA-1 (1/100, MCA970R, AbD Serotec Bio-Rad, Raleigh, NC), Iba-1 (1/500, 019-19741, Wako Chemicals, Cape Charles, VA), and glial fibrillary acidic protein (GFAP) (1/500, Z0334, Dako, Burlington, Ontario, Canada). Briefly, frozen cryoprotected sections were transferred to 24-well dishes and washed 3 × 10 minutes with PBS. Sections were blocked for 1 hour at room temperature in PBS containing 3% goat serum and 0.3% Triton X-100. Sections selected for incubation with Iba-1 antibody were exposed to boiling 10 mM citrate buffer containing 0.05% Tween20 for antigen retrieval prior to blocking. All primary antibodies were diluted in the same blocking buffer and incubated overnight at 4°C. On the following morning, sections were washed 3 × 10 minutes with PBS and then incubated for 2 hours at room temperature with fluorophore-conjugated secondary antibodies diluted in the same blocking buffer. Sections were washed thoroughly in PBS, and mounted on VWR Brand frosted slides using Polyvinyl alcohol mounting medium with DABCO (made in-house) and covered with glass coverslips.

Immunochemistry sections were imaged on a Zeiss Apo-Tome.2 Microscope using StereoInvestigator (MBF, Biosciences, Williston, VT) and an air 40× objective (with numerical aperture of 0.95, and a working distance of 0.25 mm; Zeiss, Oberkochen, Germany). Binary images were generated in ImageJ (National Institutes of Health, Bethesda, MD) to estimate the percent area occupied by stained cells. A Sobel edge detection filter was first applied to calculate local derivatives along each imaging axis. The edge-enhanced image was then computed by quadrature summation of the two derivatives. Next, images were blurred with a Gaussian filter (kernel size of 3 pixels), and the background subtracted (using a sliding paraboloid of 50 pixels). Finally, images were binarized using the Make Binary algorithm in ImageJ, at a set threshold so that the fractional area occupied by positively stained cells could be computed. The fractional area occupied by positively stained GFAP and Iba-1 cells was compared between groups across all brain sections (with ventricles excluded by manual segmentation). The NeuN and RECA-1 staining was examined in the perilesional ROI, which was defined by directly projecting manually segmented areas of intense cortical staining on GFAP and Iba-1 in adjacent brain sections.

Statistical Analysis

Linear mixed effect (LME) modeling (http://www.R-project.org) was used in the statistical analysis, as it is particularly well suited for the present data since it recognizes the relationship between serial observations on the same subjects while allowing for unbalanced groups (here present due to attrition). LME thus produces robust and sensible restricted maximum likelihood estimates in the presence of unbalanced allocation of subjects by factor. Lesion volume, average resting perfusion, and average perfusion response to hypercapnia were modeled as linear functions of hemisphere (peri- vs. contralesional), group (placebo vs. FR122047) and time after stroke (7 vs. 21 days). The fractional area of perilesional tissue occupied by cells stained for NeuN, and RECA-1; and the fractional area occupied by Iba-1 and GFAP-positive cells were modeled as linear functions of group (placebo vs. FR122047). Subjects were treated as random effects, thus accounting for across-subject variation.

Results

Resting Perfusion and Vascular Reactivity to Hypercapnia

Maps of representative resting perfusion and perfusion responses to hypercapnia are shown in Figs. 1a,b and 2a,b, along with plots of the mean groupwise signal within contra- and perilesional ROIs (Figs. 1c, 2c) and the interhemispheric cortical signal ratios (Figs. 1d, 2d). All averaged resting perfusion and perfusion responses to hypercapnia (mean ± SEM, in percent) are listed in Table 1. The peri-

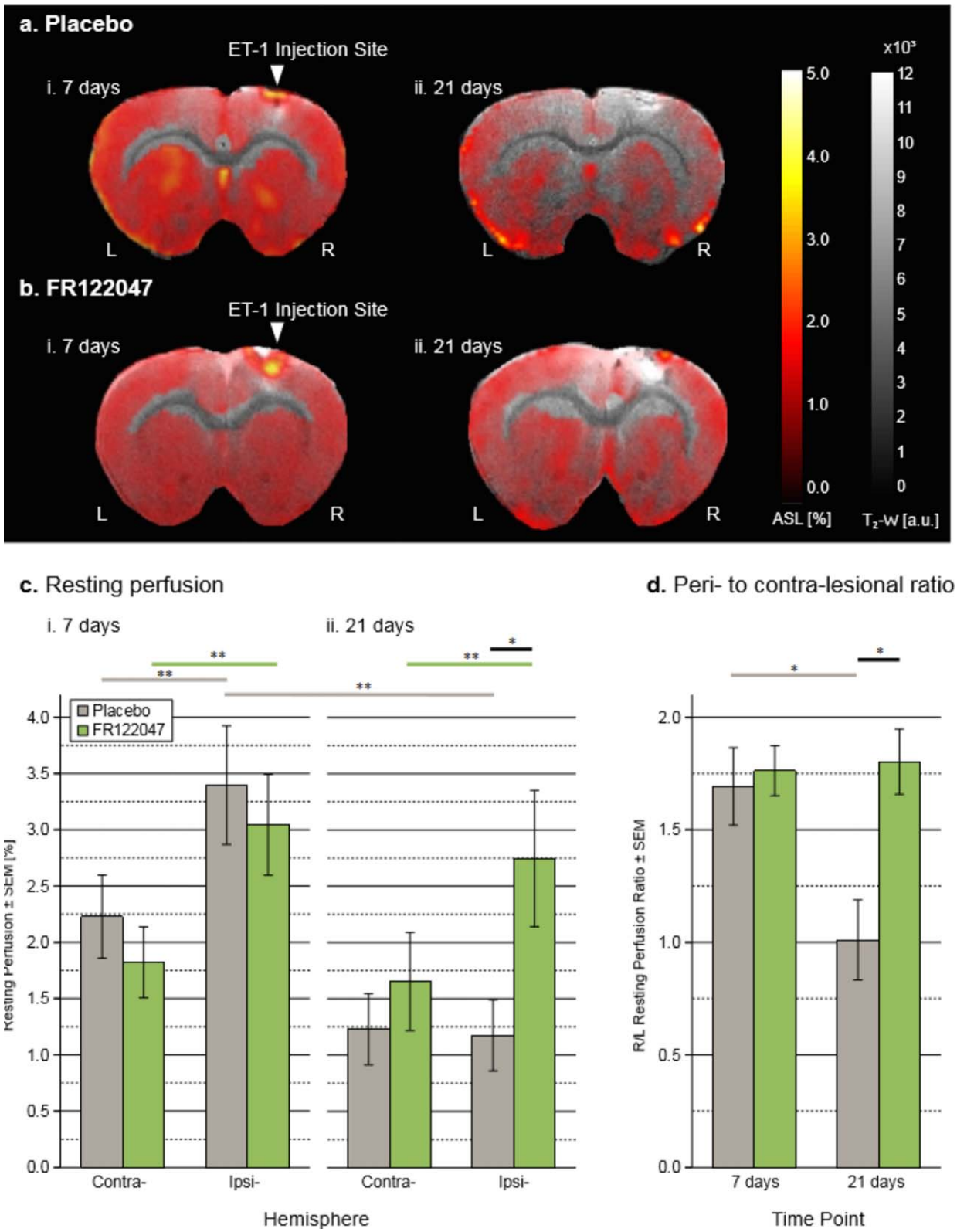

FIGURE 1: Resting perfusion: Representative maps of resting perfusion from a placebo (**a**) and FR122047-treated rat (**b**) at 7 (i) and 21 (ii) days after stroke. The resting perfusion (mean ± SEM) in contra- and perilesional ROIs are plotted in (**c**) for 7 days (i) ($n = 9$ placebo, and $n = 10$ FR122047-treated rats) and 21 days (ii) ($n = 7$ placebo, and $n = 9$ FR122047-treated rats). The interhemispheric resting perfusion ratio (R/L, right normalized to left) is plotted in (**d**). Placebo rats' data are plotted in gray and FR122047-treated rats' data in green. Statistically significant differences are indicated with horizontal lines above the bar-graphs in (c,d): the color of the bar indicates the groups being compared (gray: controls, green: FR122047-treated animals, black: controls vs. FR122047-treated animals). Resting perfusion was elevated 7 days poststroke peri- vs. contralesionally in both groups ($P < 0.01$). At 21 days after intervention there was no longer a difference in resting perfusion between hemispheres in placebo rats ($P = 0.8$). In contrast, the perilesional cortex of FR122047-treated rats remained hyperperfused ($P = 0.006$). Furthermore, resting perfusion was greater in the perilesional ROI in FR122047 relative to placebo rats ($P = 0.05$). Across time, placebo rats showed a decrease in perilesional resting perfusion ($P = 0.01$), whereas FR122047-treated rats showed no change ($P = 0.7$). By 21 days, the interhemispheric ratio within placebo rats had decreased ($P = 0.03$), whereas there was no time-dependent change in the interhemispheric ratio of FR122047-treated rats ($P = 0.8$). No changes were observed in contralesional perfusion in either group. (*$P < 0.05$, **$P < 0.01$).

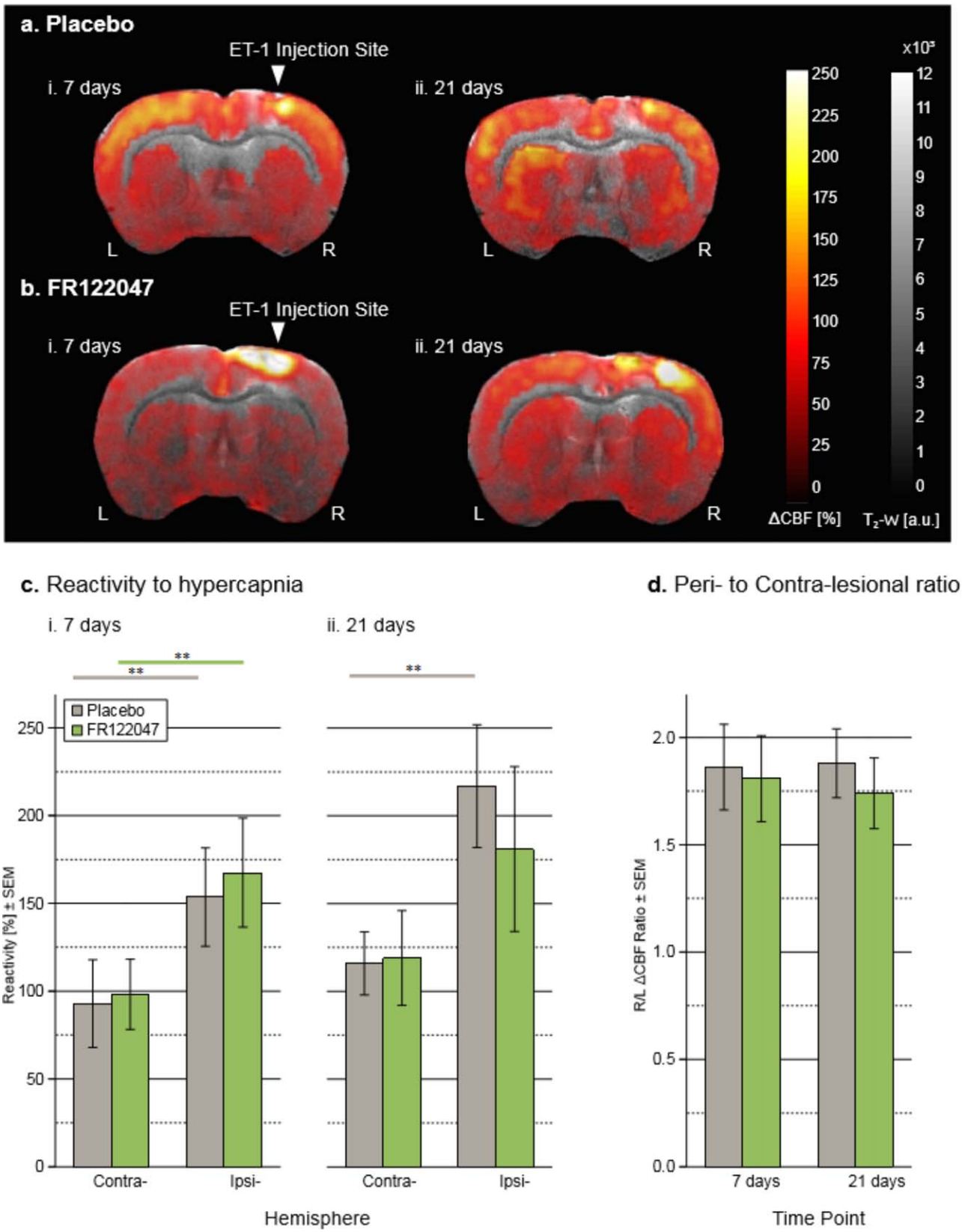

FIGURE 2: Hypercapnia-elicited changes in blood flow: Representative maps of reactivity to hypercapnia from a placebo (**a**) and FR122047-treated rat (**b**) at 7 (i) and 21 (ii) days after stroke. The perfusion change elicited by hypercapnia in contra- and perilesional ROIs are plotted in (**c**) for 7 days (i) ($n = 9$ placebo, and $n = 8$ FR122047-treated rats) and 21 days (ii) ($n = 6$ placebo, and $n = 9$ FR122047-treated rats). The interhemispheric ratio of perfusion responses is plotted in (**d**). Placebo rats' data are plotted in gray and FR122047-treated rats' data in green. Statistically significant differences are indicated with horizontal lines above the bar-graphs in (c,d): the color of the bar indicates the groups being compared (gray: controls, green: FR122047-treated animals). At 7 days poststroke, perilesional vascular reactivity to hypercapnia was elevated, in comparison to the contralesional levels, in both groups ($P < 0.002$). At 21 days after stroke, perilesional perfusion responses to hypercapnia were elevated ($P = 0.005$), while FR122047-treated rats no longer showed lateralization ($P = 0.2$). However, there were no significant differences between groups, nor were there time-dependent differences in either hemisphere in either group. (*$P < 0.05$, **$P < 0.01$).

TABLE 1. Mean Signal ± SEM [%] for Resting Perfusion, and Perfusion Response to Hypercapnia in Placebo-Administered and FR122047-Treated Rats Before (7 Days) and After (21 Days) Intervention in the Perilesional ROI (Right) and in the Contralesional ROI (Left)

Day	Placebo			FR122047		
	Left [%]	Right [%]	Ratio [R/L]	Left [%]	Right [%]	Ratio [R/L]
Resting perfusion						
7	2.2 ± 0.4	3.4 ± 0.5	1.7 ± 0.2	1.8 ± 0.3	3.0 ± 0.4	1.8 ± 0.1
21	1.2 ± 0.3	1.2 ± 0.3	1.0 ± 0.2	1.7 ± 0.4	2.7 ± 0.6	1.8 ± 0.1
Perfusion response to hypercapnia						
7	93 ± 25	154 ± 28	1.9 ± 0.2	98 ± 20	168 ± 31	1.8 ± 0.2
21	116 ± 18	217 ± 35	1.9 ± 0.2	119 ± 27	181 ± 47	1.7 ± 0.2

The interhemispheric ratio ([R/L] right normalized to left) is reported in columns 4 and 7. For each rat, the mean signal within the peri- and contralesional ROI was estimated along with the interhemispheric ratio.

to contralesional ratios (listed in Table 1 and plotted in Figs. 1d and 2d) were computed in each rat and averaged within groups to facilitate intersubject comparisons given variability in labeling coil placement in relation to the carotids and subjects' responses to anesthesia. Prior to intervention, there were no differences between groups in lesion volume ($P = 0.6$), resting perfusion ($P = 0.7$), or perfusion responses to hypercapnia ($P = 0.6$).

RESTING PERFUSION. In both groups, at 7 days resting perfusion was elevated peri- vs. contralesionally: 3.4 ± 0.5% vs. 2.2 ± 0.4% in placebo ($n = 9$, $P = 0.01$) and 3.0 ± 0.4% vs. 1.8 ± 0.03% in FR122047-treated rats ($n = 10$, $P = 0.0001$, Fig. 1c.i). Across all animals, perilesional perfusion was 170 ± 10% contralesional perfusion at 7 days (Fig. 1d). Following intervention at 21 days, resting perfusion was no longer lateralized in placebo rats: 1.2 ± 0.3% in both hemispheres ($n = 7$, $P = 0.8$, Fig. 1c.ii). In contrast, resting perfusion in FR122047-treated rats remained elevated peri- vs. contralesionally: 2.7 ± 0.6% vs. 1.7 ± 0.4% ($n = 9$, $P = 0.006$, Fig. 1c.ii). Furthermore, resting perfusion was greater in the perilesional ROI of FR122047-treated rats relative to placebo rats ($P = 0.05$). Across time, the placebo group exhibited a decrease in perilesional resting perfusion: from 3.4 ± 0.5% at 7 vs. 1.2 ± 0.3% by 21 days ($P = 0.01$, Fig. 1c), whereas FR122047-treated rats showed no time-dependent changes ($P = 0.6$, Fig. 1c). No changes in resting perfusion were observed in the contralesional ROI in either group across time (placebo: $P = 0.1$, and FR122047: $P = 0.7$, Fig. 1c).

PERFUSION RESPONSES. In response to hypercapnia, perilesional vascular reactivity was almost doubled 7 days poststroke peri- vs. contralesionally: 154 ± 28% vs. 93 ± 25% in placebo animals ($n = 9$, $P = 0.0009$); and 168 ± 31% vs. 98 ± 20% in FR122047-treated rats ($n = 8$, $P = 0.002$, Fig. 2c.i). Across all animals, perfusion increases in response to hypercapnia was 180 ± 10% of the contralesional level at 7 days (Fig. 2d). At 21 days poststroke, perilesional perfusion responses to hypercapnia were still strongly elevated in placebo rats: 217 ± 35% peri- vs. 116 ± 18% contralesionally ($n = 6$, $P = 0.005$, Fig. 2c.ii). In contrast, FR122047-treated rats showed no lateralization of perfusion responses to hypercapnia: 181 ± 47% vs. 119 ± 27% ($n = 9$, $P = 0.2$, Fig. 2c.ii). However, there were no significant differences between groups in peri- ($P = 0.7$ at 7 and $P = 0.6$ at 21 days) or contralesional ($P = 0.9$ at 7 and $P = 0.9$ at 21 days) hemispheres at either timepoint, nor did perfusion response changes depend on treatment group in contra- ($P = 0.9$) or ipsilateral ($P = 0.4$) hemispheres (Fig. 2c).

Immunohistochemistry

Representative Iba-1 and GFAP images from a placebo and an FR122047-treated rat are shown in Fig. 3, along with the mean ± SEM Iba-1 and GFAP fractional areas. The corresponding NeuN and RECA-1 data are shown in Fig. 4. The fractional area occupied by microglia/macrophages was smaller in FR122047-treated than in placebo rats: 17 ± 1% in FR122047 vs. 20 ± 1% in placebo rats ($P = 0.05$) 21 days poststroke (Iba-1 Fig. 3b). The fractional area occupied by astrocytes was not different between the two groups: 38 ± 2% in FR122047 vs. 43 ± 4% in placebo rats ($P = 0.4$, GFAP Fig. 3b). $NeuN^+$ cells occupied a smaller cortical area peri- vs. contralesionally: 14.9 ± 0.8% peri- vs. 32 ± 3% contralesionally in placebo ($P = 0.03$); and 22 ± 1% peri- vs. 36 ± 2% contralesionally in FR122047-treated rats ($P = 0.009$). However, FR122047-treated rats showed increased perilesional neuronal survival: the fractional area occupied by neurons was greater in FR122047-treated rats relative to that of placebo rats ($P = 0.02$, NeuN Fig. 4b). Perilesional angiogenesis was observed in both

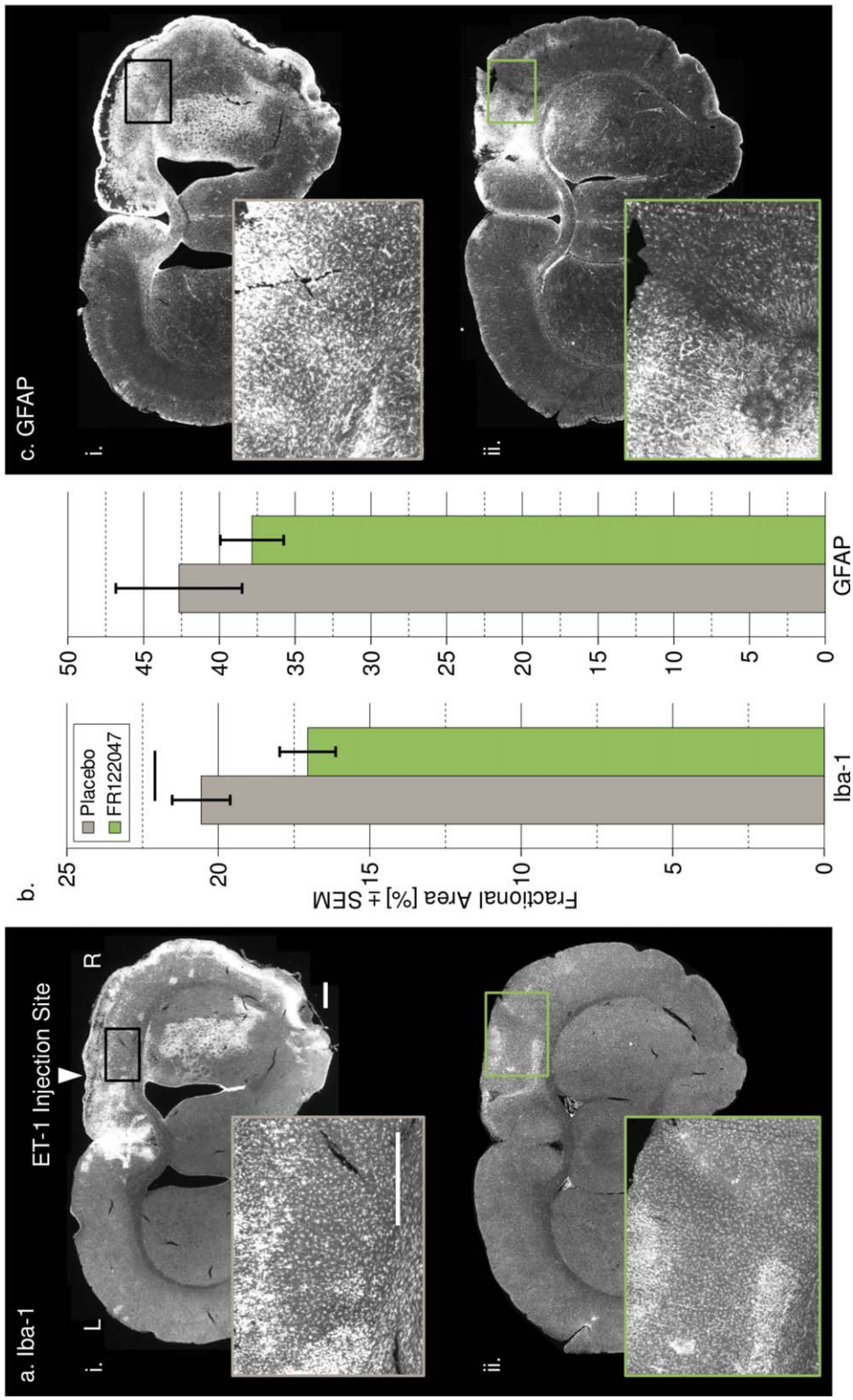

FIGURE 3: Iba-1 and GFAP immunohistochemistry: Representative Iba-1 images from a placebo rat (i) and from an FR122047-treated rat (ii) are shown in (a). Representative GFAP images from neighboring coronal sections are shown in (c). The average Iba-1 and GFAP-positive fractional areas across rats for both groups are plotted in (b). The fractional area occupied by microglia/macrophages (Iba-1) was smaller in FR122047-treated relative to that in placebo-administered rats: 17.1 ± 0.9% in FR122047-treated vs. 20 ± 1% in placebo rats ($P = 0.05$). Scale bars: 1 mm.

groups: endothelial cells occupied a greater fractional area peri- vs. contralesionally (Supplementary Fig. 2), with 51 ± 2% peri- vs. 22 ± 1% contralesionally in placebo ($P = 0.006$), and 49 ± 3% peri- vs. 22 ± 2% contralesionally in FR122047-treated rats ($P = 0.003$). There was no effect of group on the fractional area occupied by endothelial cells

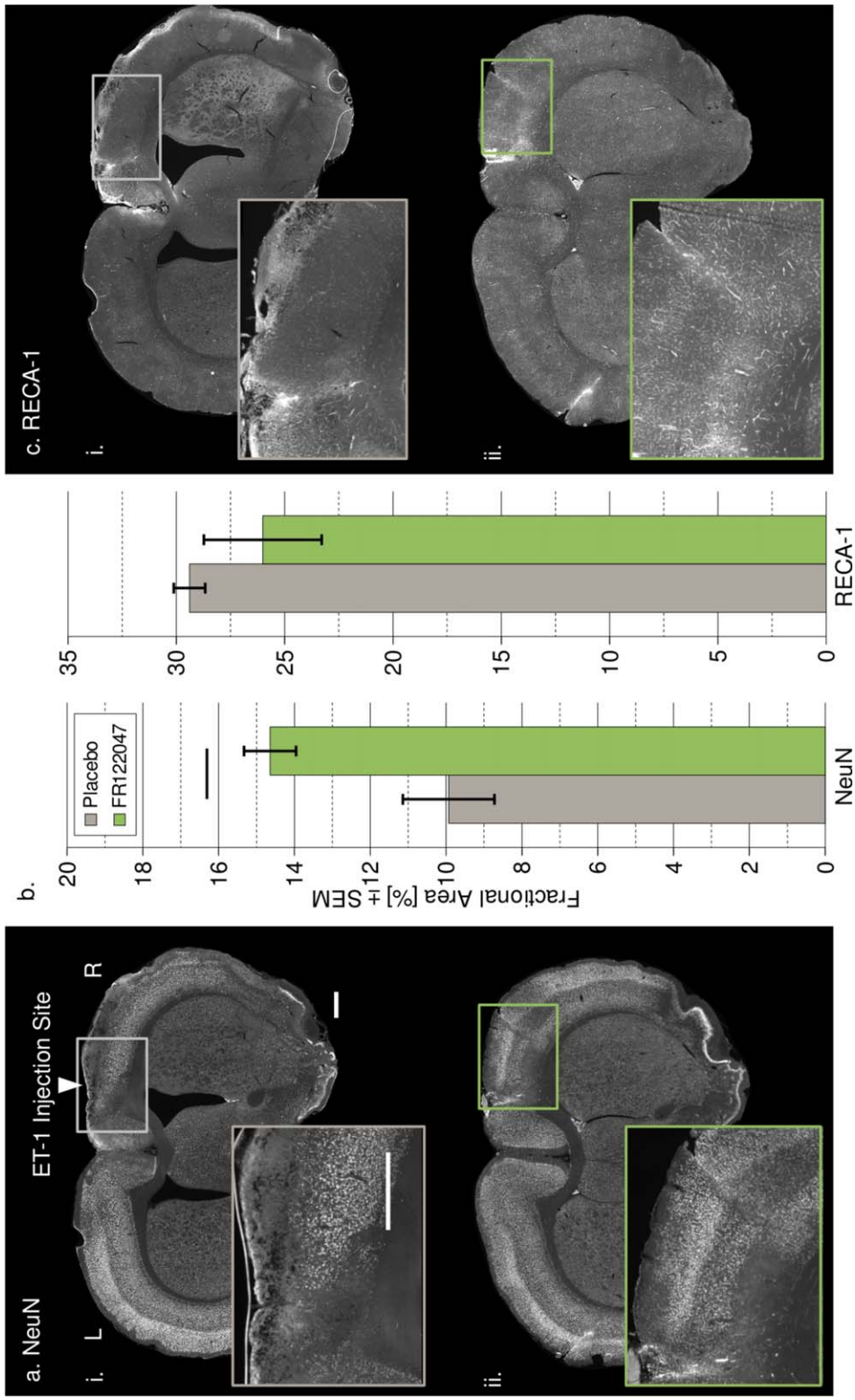

FIGURE 4: NeuN and RECA-1 immunohistochemistry: Representative NeuN images from a placebo rat (i) and from an FR122047-treated rat (ii) are shown in (a). Representative RECA-1 images from neighboring coronal sections are shown in (c). The average fractional areas occupied by neurons and endothelial cells are plotted in (b). FR122047-treated rats showed greater perilesional neuronal survival than did the placebo rats: 14.7 ± 0.7% of perilesional cortex was occupied by $NeuN^+$ cells in FR122047-treated vs. 10 ± 1% in placebo rats ($P = 0.02$). Scale bars: 1 mm.

($P = 0.3$). (In addition, the average stroke volume on T_2-weighted MRI at 7 days poststroke in rats analyzed with immunohistochemistry was $50 \pm 10\,mm^3$, $n = 7$, with no differences between groups: $56 \pm 20\,mm^3$ in placebo, $n = 3$ vs. $44 \pm 11\,mm^3$ in FR122047-treated rats, $n = 4$; Supplementary Table 3.)

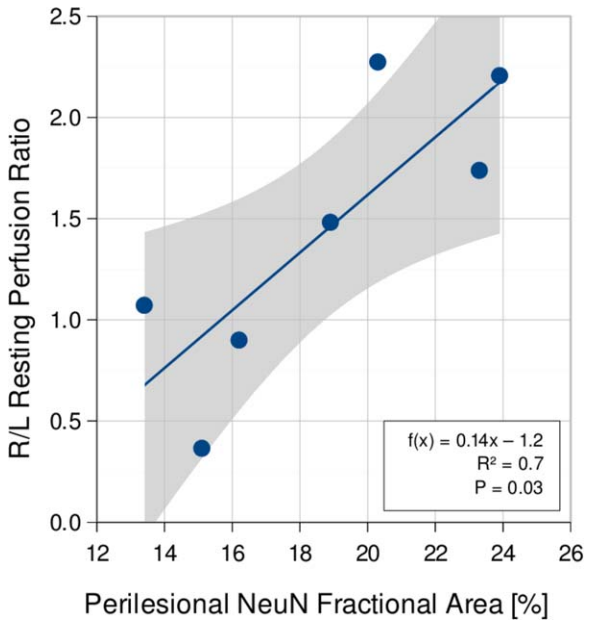

FIGURE 5: Perilesional perfusion and neuronal survival. The peri- relative to contralesional resting perfusion ratio at 21 days is plotted against the fractional area (%) occupied by neuronal cells within the perilesional ROI in the same animals, at the same timepoint. Perilesional resting hyperperfusion increased with increasing perilesional neuronal survival (slope = 0.14 ± 0.05; $R^2 = 0.7$, $P = 0.03$).

Correlation of Resting Perfusion and Immunohistochemistry

In Fig. 5, the peri- vs. contralesional resting perfusion ratio is plotted against the fractional area occupied by neurons within the perilesional ROI. The resting perfusion lateralization increased with increasing perilesional neuronal survival (slope = 0.14 ± 0.05; $R^2 = 0.7$, $P = 0.03$). Further, there was a trend toward an increase in resting perfusion with decreasing microglia/macrophages recruitment (slope = –0.15 ± 0.09: $R^2 = 0.4$, $P = 0.1$).

Discussion

The present study characterized neurogliovascular changes elicited by selective COX-1 inhibition via intracerebroventricular FR122047-treatment initiated 7 days following stroke in an endothelin-1 model of focal ischemia. Stroke induced a transient increase in perilesional resting perfusion and a sustained elevation in perilesional vascular reactivity to hypercapnia in placebo rats. In FR122047-treated rats, perilesional hyperperfusion persisted at 21 days poststroke, while perfusion responses to hypercapnia showed a tendency to normalize (a statistically significant difference between hemispheres at 7 days did not persist at 21 days). However, the interhemisphere ratio in the treated group at 21 days remained above 1 and did not change between 7 and 21 days. The former result arose due to the increase in perfusion response variability ipsilesionally observed in the treated animals between 7 and 21 days. Increased variability could indicate the presence of responders and nonresponders within the treated group.

Immunohistochemistry revealed perilesional neuronal loss, increased perilesional endothelial density, and widespread increases in microglial/macrophage recruitment and astrocytic reactivity in all rats. Briefly, NeuN stains the DNA-binding, neuron-specific protein NeuN found in neuronal cells in the central nervous system (CNS) (EMD Millipore). RECA-1 stains the cell surface antigen RECA-1 expressed by all endothelial cells (AbD Serotec Bio-Rad). Anti-Iba-1 is an unconjugated polyclonal antibody that binds ionizing calcium-binding adaptor molecule 1 (Iba-1): an actin-binding protein uniquely expressed by microglial/macrophages (Wako Chemicals). Finally, astrocytic reactivity was measured with anti-GFAP (Z0334), which binds GFAP to label astrocytes in the CNS (Dako). Relative to placebo rats, FR122047-treated rats showed increased perilesional neuronal survival and decreased perilesional microglial/macrophage recruitment. Furthermore, greater perilesional neuronal survival was associated with increased peri- relative to contralesional perfusion.

At 1 week poststroke, across all rats, perilesional perfusion and perfusion responses to hypercapnia were significantly above respective contralesional levels. These elevations are consistent with previous reports in rat models of focal ischemic injury,[27–29] but in contrast with other studies.[29,30] In a rat transient occlusion model of stroke, perilesional hyperperfusion is observed 2–4 days following ischemia.[27] In a 2-hour intraluminal middle cerebral artery occlusion (MCAO) model of focal ischemia, the 7-day perilesional perfusion is double that of sham-operated rats,[28] in excellent agreement with the present finding. Further, in a rat 60-minute transient MCAO model, Wegener et al[29] identified three outcome patterns. 1) Large hemispheric cortico-subcortical strokes, with hyperperfusion on day 4 poststroke and a further increase in resting perfusion on day 14, with decreased vasoreactivity at both timepoints. 2) Moderate cortico-subcortical strokes, with maximal hyperperfusion on day 4, decreased vasoreactivity on day 4, and elevated vasoreactivity on day 14. 3) Predominantly subcortical infarctions, with maximal hyperperfusion on day 1; persistent hyperperfusion on day 14, and unaffected or increased vasoreactivity in punctate areas within the ischemic lesion on day 4, and more pronounced hyperreactivity by day 14. Although somewhat variable, prior work in preclinical models of focal ischemia provides evidence of perilesional hyperperfusion and hyperreactivity to hypercapnia during the subacute period, in agreement with the present work.

On the other hand, Shen et al report that hyperperfusion peaks 48 hours after MCAO and resolves by day 7 in most rats. The detection of hyperperfusion in this study is, however, strongly dependent on occlusion time (30/60/90 min)[30]: hyperperfusion is detected (at least once) in all of

the short, in half of the mid-length, and in none of the long occlusion time groups[30] (shorter MCAO times have been suggested less likely to damage blood vessels). Furthermore, they observed that hypercapnia decreases perfusion response to hypercapnia at 48 hours within the hyperperfused perilesional tissue relative to the contralesional perfusion response.[30] Presently observed hyperperfusion at 7 days was, in contrast, accompanied by increased perilesional perfusion responses to hypercapnia: due to the highly dynamic changes in the perilesional vascular function during the first week following stroke, the interpolation of present 7-day findings to a 2-day timepoint is exceedingly difficult and likely accounts for the discrepancy.

In this work, elevated resting perfusion likely resulted from increased vascular density due to injury-induced angiogenesis, which has been widely observed histologically following focal ischemia in rats.[28–32] Previous work shows an increase in the number of endothelial cells ($CD31^+$) between 2 and 7 days following focal ischemia.[28] Further, perilesional RECA-1 staining at 140% the contralesional level in rats with evidence of increased vasoreactivity has been observed, whereas rats with normal perfusion responses to hypercapnia exhibited no lateralization in RECA-1 staining.[29] Likewise, blood vessel branch number (using RECA-1 staining) at 140% the contralesional level concomitant to hyperperfusion up to 12 weeks following MCAO has been reported.[32] In addition, it has been observed that the density of perilesional small caliber vessels ($<30\ \mu$m) 3 days after stroke are three times the density seen in sham-operated controls.[31] Of note, vascular networks formed by vessel sprouting undergo extensive pruning to form a mature network[33] and prior work in a rat model of MCAO suggests that angiogenesis following focal ischemia begins with the hyperdilation of perilesional vessels and subsequent generation of microvessels during the weeks following ischemic injury.[34] In the present work, RECA-1 immunohistochemical analysis indicated doubling of perilesional vascular density relative to contralesional levels in all animals (Supplementary Fig. 2). The increase in perilesional perfusion observed in all rats prior to intervention was thus consistent with ischemia-induced angiogenesis. Notably, histopathological analysis demonstrates poststroke angiogenesis in patients, and the degree of angiogenesis correlates with better functional outcome and longer survival following stroke.[35–37] Further, elevation of anti-angiogenesis factors in blood (eg, thrombospondin-1) predicts poor long-term outcome and is associated with higher mortality.[38]

Increased perilesional neuronal survival in FR122047-treated rats likely resulted from attenuation of secondary cell death, which has been reported previously 1–3 weeks following focal ischemia.[39] In support of this assertion, COX-1 inhibition (via valeryl salicylate, 20 mg/kg, administered intraperitoneally 6 hours postreperfusion) decreases neuronal loss in a gerbil model of global ischemia.[20] This effect has been suggested to result from a reduction in PG-D_2 production—largely mediated by COX-1 postischemia[16]—that reduces the PG-D_2-induced increase in neuronal apoptosis by activation of poly ADP ribose polymerase and caspase-3.[9]

Pruning, recruitment of mural cells, the generation of an extracellular matrix, specialization of the vessel wall, and the functional integration of nascent vasculature are highly dependent on the spatiotemporal interaction of nascent vessels with surrounding neurons and glia.[33] Increased perilesional neuronal survival may thus have promoted the integration and maturation of the nascent perilesional vessels, hence contributing to persistent perilesional hyperperfusion in FR122047-treated rats. This hypothesis is further buttressed by the correlation between resting perfusion lateralization and perilesional neuronal survival. In contrast, greater perilesional neuronal loss in the placebo rats may have led to more extensive pruning during the maturation of the nascent vessels, thus rendering some of them nonperfused,[33] accounting for the reduction in perilesional perfusion with time in the placebo animals. Perilesional hyperreactivity to hypercapnia similarly may have been due to the lower resistance of nascent vessels.[40] Persistent perilesional hyperperfusion in treated rats may have also been influenced by an FR122047-mediated reduction in PGs that promote vasoconstriction and are predominately produced via COX-1 in activated microglia,[6] whose perilesional density was decreased in FR122047-treated relative to placebo rats.

Although the present work indicates beneficial effects of COX-1 inhibition in the subacute phase following focal ischemic stroke, the development of such a strategy for clinical populations warrants further investigation. In particular, the current study was limited with respect to the number of animals examined (particularly due to attrition incurred from longitudinal observations), the duration of the observation period, and the lack of behavioral analyses. The consequences of increased neuronal survival presently evaluated ex vivo in FR122047-treated animals should be further investigated by an in vivo characterization of perilesional neuronal function. Examining outcomes at multiple chronic timepoints—preferably a full month postintervention—is necessary for assessing long-term outcome. Finally, a battery of behavioral testing is required for a comprehensive evaluation of functional outcome.

In conclusion, the present study provided evidence of beneficial effects of delayed selective COX-1 inhibition on the neurogliovascular unit in the peri-infarct zone. Treatment resulted in increased perilesional neuronal survival, decreased recruitment of microglia/macrophages, and sustained elevation in perilesional perfusion. These histopathological and imaging findings warrant further investigation of the effect of selective COX-1 inhibition on functional

outcome in the chronic stage of stroke recovery. Furthermore, future measurements of PGs levels post-COX-1 inhibition, along with in vivo measurements of changes in vascular architecture and function, as well as neuronal excitability, will further the mechanistic understanding of the observed effects.

Acknowledgment

Contract grant sponsor: Canadian Institute for Health Research; contract grant numbers: MOP 123411; 264623

References

1. Teasell R, Rice D, Richardson M, et al. The next revolution in stroke care. Expert Rev Neurother 2014;14:1307–1314.
2. Hackett ML, Duncan JR, Anderson CS, Broad JB, Bonita R. Health-related quality of life among long-term survivors of stroke: results from the Auckland Stroke Study, 1991-1992. Stroke 2000;31:440–744.
3. Kim JK, Kawabori M, Yenari MA. Innate inflammatory responses in stroke: mechanisms and potential therapeutic targets. Curr Med Chem 2014;21:2076–2097.
4. Iadecola C, Anrather J. The immunology of stroke: from mechanisms to translation. Nat Med 2011;17:796–808.
5. Stanimirovic D, Satoh K. Inflammatory mediators of cerebral endothelium: a role in ischemic brain inflammation. Brain Pathol 2000;10:113–126.
6. Yagami T, Koma H, Yamamoto Y. Pathophysiological roles of cyclooxygenases and PG in the central nervous system. Mol Neurobiol 2015: 1–18.
7. Kawano T, Anrather J, Zhou P, et al. Prostaglandin E2 EP1 receptors: down-stream effectors of COX-2 neurotoxicity. Nat Med 2006;12:225–229.
8. Saleem S, Ahmad AS, Maruyama T, Narumiya S, Doré S. PGF(2alpha) FP receptor contributes to brain damage following transient focal brain ischemia. Neurotox Res 2009;15:62–70.
9. Liu H, Li W, Rose ME, et al. Prostaglandin D2 toxicity in primary neurons is mediated through its bioactive cyclopentenone metabolites. Neurotoxicology 2013;39:35–44.
10. Félétou M, Huang Y, Vanhoutte PM. Endothelium-mediated control of vascular tone: COX-1 and COX-2 products. Br J Pharmacol 2011;164: 894–912.
11. Sanchez-Moreno C, Dashe JF, Scott T, Thaler D, Folstein MF, Martin A. Decreased levels of plasma vitamin C and increased concentrations of inflammatory and oxidative stress markers after stroke. Stroke J Cereb Circ 2004;35:163–168.
12. Ott E, Nussmeier NA, Duke PC, et al. Efficacy and safety of the cyclooxygenase 2 inhibitors parecoxib and valdecoxib in patients undergoing coronary artery bypass surgery. J Thorac Cardiovasc Surg 2003; 125:1481–1492.
13. Nussmeier NA, Whelton AA, Brown MT, et al. Complications of the COX-2 inhibitors parecoxib and valdecoxib after cardiac surgery. N Engl J Med 2005;352:1081–1091.
14. Cannon CP, Curtis SP, FitzGerald GA, et al. Cardiovascular outcomes with etoricoxib and diclofenac in patients with osteoarthritis and rheumatoid arthritis in the multinational etoricoxib and diclofenac arthritis long-term (MEDAL) programme: a randomized comparison. Lancet 2006;368:1771–1781.
15. Perrone MG, Scilimati A, Simone L, Vitale P. Selective COX-1 inhibition: a therapeutic target to be reconsidered. Curr Med Chem 2010; 17:3769–3805.
16. Song WL, Wang M, Ricciotti E, et al. Tetranor PGDM, an abundant urinary metabolite reflects biosynthesis of prostaglandin D2 in mice and humans. J Biol Chem 2008;283:1179–1188.
17. Kobayashi T, Tahara Y, Matsumoto M, et al. Roles of thromboxane A(2) and prostacyclin in the development of atherosclerosis in apoE-deficient mice. J Clin Invest 2004;114:784–794.
18. McAdam BF, Catella-Lawson F, Mardini IA, Kapoor S, Lawson JA, FitzGerald GA. Systemic biosynthesis of prostacyclin by cyclooxygenase (COX)-2: the human pharmacology of a selective inhibitor of COX-2. Proc Natl Acad Sci U S A 1999;96:272–277.
19. Iadecola C, Sugimoto K, Niwa K, Kazama K, Ross ME. Increased susceptibility to ischemic brain injury in cyclooxygenase-1-deficient mice. J Cereb Blood Flow Metab 2001;21:1436–1441.
20. Candelario-Jalil E, González-Falcón A, García-Cabrera M, et al. Assessment of the relative contribution of COX-1 and COX-2 isoforms to ischemia-induced oxidative damage and eurodegeneration following transient global cerebral ischemia. J Neurochem 2003;86:545–555.
21. Windle V, Szymanska A, Granter-Button S, et al. An analysis of four different methods of producing focal cerebral ischemia with endothelin-1 in the rat. Exp Neurol 2006;201:324–334.
22. Carmichael T. Rodent models of focal stroke: size, mechanism and purpose. NeuroRx 2005;2:396–409.
23. ImageMagick Studio LLC. http://www.imagemagick.org/script/index.php. Copyright 1999-2013 Non-profit organization dedicated to making software imaging solutions freely available. 2013.
24. van der Zijden JP, van der Toorn A, van der Marel K, Dijkhuizen RM. Longitudinal in vivo MRI of alterations in perilesional tissue after transient ischemic stroke in rats. Exp Neurol 2008;212:207–212.
25. Lake EM, Chaudhuri J, Thomason L, et al. The effects of delayed reduction of tonic inhibition on ischemic lesion and sensorimotor function. J Cereb Blood Flow Metab 2015;35:1601–1609.
26. Kang JK, Bénar C, Al-Asmi A, et al. Using patient-specific hemodynamic response functions in combined EEG-fMRI studies in epilepsy. Neuroimage 2003;20:1162–1170.
27. Wang L, Yushmanov VE, Liachenko SM, Tang P, Hamilton RL, Xu Y. Late reversal of cerebral and water diffusion after transient focal ischemia in rats. J Cereb Blood Flow Metab 2002;22: 253–261.
28. Martin A, Macé E, Boisgard R, et al. Imaging of perfusion, angiogenesis, and tissue elasticity after stroke. J Cereb Blood Flow Metab 2012; 32:1496–1507.
29. Wegener S, Artmann J, Luft AR, Buxton RB, Weller M, Wong EC. The time of maximum post-ischemic hyperperfusion indicates infarct growth following transient experimental ischemia. PLoS One 2013;8: 1–6.
30. Shen Q, Du F, Huang S, Duong TQ. Spatiotemporal characteristics of postischemic hyperperfusion with respect to changes in T1, T2, diffusion, angiography, and blood-brain barrier permeability. J Cereb Blood Flow Metab 2011;31:2076–2085.
31. Lin CY, Chang C, Cheung WM, et al. Dynamic changes in vascular permeability, cerebral blood volume, vascular density, and size after transient focal cerebral ischemia in rats: evaluation with contrast-enhanced magnetic resonance imaging. J Cereb Blood Flow Metab 2008;28:1491–1501.
32. Hayward NM, Yanev P, Haapasalo A, et al. Chronic hyperperfusion and angiogenesis follow subacute hypo-perfusion in the thalamus of rats with focal cerebral ischemia. J Cereb Blood Flow Metab 2011;31: 1119–1132.
33. Korn C, Augustin HG. Mechanisms of vessel pruning and regression. Dev Cell 2015;34:5–17.
34. Morris DC, Yeich T, Khalighi MM, Soltanian-Zadeh H, Zhang ZG, Chopp M. Microvascular structure after embolic focal cerebral ischemia in the rat. Brain Res 2003;972:31–37.

35. Krupiński J, Kaluza J, Kumar P, Kumar S, Wang JM. Some remarks on the growth-rate and angiogenesis of microvessels in ischemic stroke. Morphometric and immunocytochemical studies. Patol Pol 1993;44: 203–209.

36. Krupiński J, Kaluza J, Kumar P, Kumar S, Wang JM. Role of angiogenesis in patients with cerebral ischemic stroke. Stroke 1994;25: 1794–1798.

37. Szpak FM, Lechowicz W, Lewandowska E, Bertrand E, Wierzba-Bobrowicz T, Dymecki J. Border zone neovascularization in cerebral ischemic infarct. Folia Neuropathol 1999;37:264–268.

38. Gao JB, Tang WD, Wang HX, Xu Y. Predictive value of thrombospondin-1 for outcomes in patients with acute ischemic stroke. Clin Chim Acta 2015;450:176–180.

39. Wegener S, Weber R, Ramos-Cabrer P, et al. Temporal profile of T2-weighted MRI distinguishes between pannecrosis and selective neuronal death after transient focal cerebral ischemia in the rat. J Cereb Blood Flow Metab 2006;26:38–47.

40. White FC, Bloor CM. Coronary vascular remodeling and coronary resistance during chronic ischemia. Am J Cardiovasc Pathol 1992;4: 193–202.